

Available online at [www.sciencedirect.com](http://www.sciencedirect.com)**SciVerse ScienceDirect**

Procedia Engineering 41 (2012) 1135 – 1144

---

**Engineering  
Procedia**


---

[www.elsevier.com/locate/procedia](http://www.elsevier.com/locate/procedia)

International Symposium on Robotics and Intelligent Sensors 2012 (IRIS 2012)

**Ant Colony Based Model Prediction of a Twin Rotor System**S. F. Toha<sup>a</sup>, S. Julai<sup>b</sup>, M. O. Tokhi<sup>c</sup> \*<sup>a</sup>*Department of Mechatronics, Faculty of Engineering, International Islamic University Malaysia, Malaysia*<sup>b</sup>*Department of Mechanical, Faculty of Engineering, University Malaya, Malaysia*<sup>c</sup>*Department of Automatic Control Systems and Engineering, University of Sheffield, UK***Abstract**

Interest in biologically-inspired optimization techniques has increased due to its accurate results, fast performance and ease of use. In this paper, an ant colony optimization (ACO) technique is deployed and used for modelling a twin rotor system. The system is perceived as a challenging engineering problem due to its strong cross coupling between horizontal and vertical axes and inaccessibility of some of its states and outputs for measurements. Accurate modelling of the system is thus required so as to achieve satisfactory control objectives. It is demonstrated that ACO can be effectively used for modelling the system with highly accurate results. The accuracy of the modelling results is demonstrated through validation tests including training and test validation and correlation tests.

© 2012 The Authors. Published by Elsevier Ltd. Selection and/or peer-review under responsibility of the Centre of Humanoid Robots and Bio-Sensor (HuRoBs), Faculty of Mechanical Engineering, Universiti Teknologi MARA.

Open access under [CC BY-NC-ND license](http://creativecommons.org/licenses/by-nc-nd/4.0/).

*Keywords:* Ant colony optimisation, Parametric modelling, Twin rotor system, AutoRegressive model.

**Nomenclature**

$\varphi$	rotational angle
$\theta$	elevation angle
$u(t)$	voltage of main rotor
$y(t)$	pitch angle of the beam
$e(t)$	error
$f_{best}$	objective function
$Q$	quantity of pheromone
$\phi_{EE}$	auto correlation of residual
$\phi_{uE}$	cross-correlation

\* Corresponding author. Tel.: +603-61965705; Fax: +603-61964466.

E-mail address: [tsfauziah@iiium.edu.my](mailto:tsfauziah@iiium.edu.my)

## 1. Introduction

This paper presents an investigation on dynamic modelling of the vertical movement of a twin rotor system; a laboratory platform representing a flexible manoeuvring structure and resembles essential characteristics of an air vehicle. Although, the twin rotor system does not fly, it has a striking similarity to a helicopter, such as system nonlinearities and cross-coupled modes. The twin rotor system, therefore, can be viewed as an unconventional and complex ‘air vehicle’ and possesses formidable challenges in modelling, control design and analysis and implementation. The interest in this work stems from the fact that helicopters are highly agile, stealthy, multi-purpose and capable of executing different tasks such as surveillance, aerial mapping and inspection, which are beyond the domain of their conventional fixed-wing counterparts. These new generation air vehicles have presented a variety of unprecedented challenges and opportunities to aerodynamicists and control engineers.

System identification using input and output data from a system is essential for controller design and nonlinear models for subsequent controller evaluation. Parametric models, characterising the twin rotor system in hovering mode, have been obtained with no *a priori* knowledge of plant model order or parameters providing any insight into physical characteristics of the plant using ant colony optimisation approach. The identified model has been exhaustively validated using time and frequency domain tests in order to instill confidence in the model for their subsequent use in the controller design. The modelling procedure adopted is suitable for a class of new generation air vehicles whose dynamics are not well-understood or difficult to model from first principles.

The ant colony optimisation (ACO) metaheuristic is a multi-agent framework for combinatorial optimisation whose main components are: a set of ant-like agents, the use of memory and of stochastic decisions, and strategies of collective and distributed learning. It finds its roots in the experimental observation of a specific foraging behaviour of some ant colonies that, under appropriate conditions, are able to select the shortest path among few possible paths connecting their nest to a food site. The pheromone, a volatile chemical substance laid on the ground by the ants while walking, affecting in turn their moving decisions according to its local intensity, is the mediator of this behaviour. All the elements playing an essential role in the ant colony foraging behaviour were understood, thoroughly reverse-engineered and put to work to solve problems of combinatorial optimisation by Marco Dorigo and his co-workers in 1999 [1].

## 2. Twin Rotor System

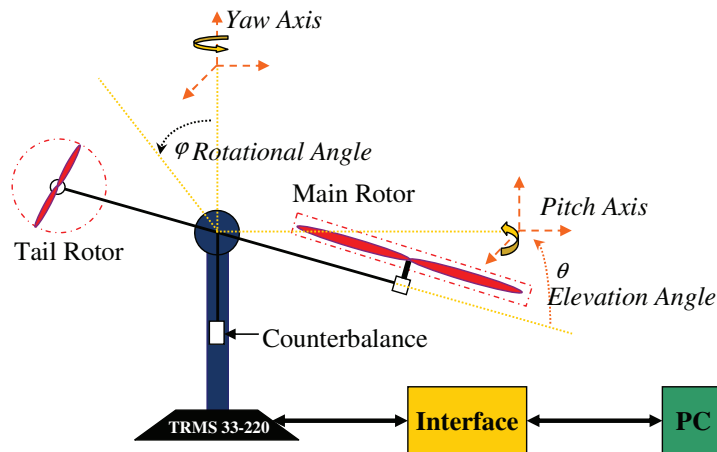


Figure 1: Twin rotor multi-input multi-output system

Research interest in laboratory set-up platforms to simulate complex aircraft manoeuvres and to investigate different control paradigms has noticeably increased in recent years. A laboratory scale aircraft fuel rig is commissioned by [2] using model based techniques to study fault diagnostic technique as high safety level within aviation. The model was developed and validated in MATLAB successfully to reduce and detect fault and failures in a highly nonlinear and complex environment such as aircraft. A fast output sampling technique for robust controller is illustrated using a laboratory scaled launch vehicle by [3]. In this approach, the fast output sampling feedback which has the features of static input feedback as well as possibility of complete pole assignment is considered. Werner and Meister proposed a 2 DOF laboratory aircraft

model, developed to model the behaviour of a vertical-take-off aircraft using a multi-modal approach for robust controller design [4]. In this work, the Linear Matrix Inequality (LMI) formulation in conjunction with convex programming for robust command tracking and disturbance rejection in normal operation as well as in failure mode is employed. This platform is quite similar to the twin rotor system. It has roll and yaw movement whereas the twin rotor system has pitch and yaw motion.

The twin rotor system is a laboratory facility retaining the most important helicopter features such as couplings and strong nonlinearities as well as it can be perceived as an unconventional and complex ‘air vehicle’. These system characteristics present formidable challenges in modelling, control design and implementation. In an actual flight situation, the parameters of a helicopter are varying due to the change in flight conditions. There is a need to perform system identification under different flight conditions in order to update the aircraft model and also the controllers. It is driven by two DC motors at both ends of the beam; the main rotor motor and tail rotor motor. Its two propellers are perpendicular to each other and joined by a beam pivoted on its base that can rotate freely in the horizontal and vertical planes. The beam can thus be moved by changing the input voltage in order to control the rotational speed of the propellers. The articulated joint allows the beam to rotate in such a way that its ends move on spherical surfaces. The system is equipped with a pendulum counterweight hanging from the beam, which is used for balancing the angular momentum. A schematic diagram of the TRMS is shown in Figure 1 and the characteristic parameters are tabulated in Table 1.

**Table 1:** Characteristic parameters of the TRMS

Parameters	Value
Maximum input voltage range	+/- 10 V
Length of the beam	0.49 m
Length of the counter balance	0.26 m
Mass of the main DC motor with main rotor	0.228 kg
Mass of the tail DC motor with tail rotor	0.206 kg

### 3. Ant Colony Optimisation (ACO)

The basic ACO algorithm actually fits a discrete problem only and is not suitable for solving continuous optimization problems such as linear or non-linear programming. Applying this algorithm to continuous domains was not straightforward where the main issue is how to model a continuous nest neighbourhood with a discrete structure. As the design problem can always be formulated as optimization problem in continuous design space, the ACO algorithm applied in any field should be modified accordingly [5-6]. Continuous ACO was proposed by Wang and Wu, [7] and Quan and Chao, [8]. This algorithm is referred to as ACO1 throughout this work. Here, the optimization problem is solved by a cooperation of artificial ant colony by exchanging information via pheromone deposited on graph edges. It consists of a framework as follows:

- Step 1      Initialization  
At the start of algorithm, the pheromone values are all initialized to a constant value (e.g.  $P_c = 1$ )
  - Step 2      Solution construction  
For each ant, the solution is constructed using pheromone trail. A constructive heuristic assembles solutions as sequences of elements from finite set of solution components.
  - Step 3      Apply pheromone update  
The pheromone update rule is used to increase the pheromone values on solution components that have been found in high quality solutions.
- Stopping criterion is imposed.

Let the vector  $X = [x_1, x_2, \dots, x_n]$  be the parameters to be optimized, where  $n$  represents the total number of parameters in the AVC system, along with upper and lower bounds to be  $x_i \in D(x_i) = [x_{i_{low}}, x_{i_{up}}]$  with  $i = 1, 2, \dots, n$ . The definition field  $D(x_i)$  is divided into  $M$  subspaces, and the middle of each subspace defines a node. A single artificial ant  $k$ ,  $k = 1, 2, \dots, n$ , where  $N_{ant}$  is the maximum number of ants, would choose to move from one node to the other, in the total of  $P$  nodes in each  $D(x_i)$ . The length of each sub-space  $h_i$  can be expressed by

$$h_i = \frac{x_{i\_up} - x_{i\_low}}{M} \tag{1}$$

For each level which has  $P$  nodes on it, there are  $M \times n$  nodes in total. A modification has been made to this algorithm by the author to the state vector of the ant  $k$  that completed its tour, as shown in Figure 2, with travel index  $[i_8, i_7, i_6, \dots, i_4]$ . This index depends on the entries of cumulative probability (CP) from the probability  $P_{ij}$ , of the ant  $k$  to move to the  $i^{\text{th}}$  node on the  $j^{\text{th}}$  level. For example if  $M = 10, CP = [0.1, 0.2, 0.3, 0.4, 0.5, 0.6, 0.7, 0.8, 0.9, 1.0]$ , and the generated random number lies between 0.7 and 0.8, the first travel index,  $i_8$ , is chosen as 8 (eighth column of the CP). This process is done until all travel index are found. The values of the parameters  $X$ , held by ant  $k$ , are as

$$[x_1, x_2, x_3, \dots, x_n] = [x_{1\_low} + i_8 \times h_1, x_{2\_low} + i_7 \times h_2, x_{3\_low} + i_6 \times h_3, \dots, x_{n\_low} + i_4 \times h_n] \tag{2}$$

The state transition rule of the ant  $k$  is expressed as

$$P_{ij} = \frac{\tau_{ij}}{\sum_{i=1}^n \tau_{ij}} \tag{3}$$

Where  $P_{ij}$ , is the probability of the ant  $k$  to move to the  $i^{\text{th}}$  node on the  $j^{\text{th}}$  level, and  $\tau_{ij}$ , is the amount of the pheromone at the node. When all the ants have finished their tours, the pheromone is updated by using

$$\tau_{ij} = (1 - \rho)\tau_{ij} + Q / f_{best} \tag{4}$$

where  $0 < \rho < 1$  is a pheromone decay parameter,  $Q$  is the quantity of pheromone laid by an ant per iteration cycle,  $\tau_0$ , is a constant for the initial value of  $\tau_{ij}$ , (for initialization  $\tau_{ij}$ , on the RHS is set to be  $\tau_0$ ), and  $f_{best}$  is the objective function value given by the best ant of each searching period.

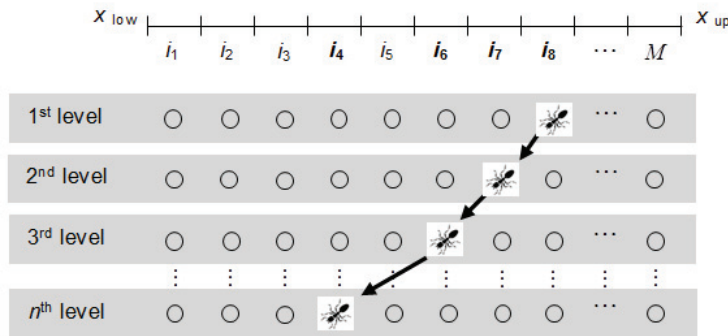


Figure 2: State space graph for ACOI

The algorithm begins with the initialization of the pheromone trail. For each ant, the desired optimization fitness function is evaluated and the minimum value is stored as  $f_0$ . At each iteration, an ant constructs a complete solution to the problem according to a probabilistic state transition rule as in equation (3). The state transition rule depends mainly on the state of the pheromone. The third step updates quantity of pheromone; a global pheromone updating rule is applied in two phases. First, an evaporation phase where a fraction of the pheromone evaporates, and then a reinforcement phase where each ant deposits an amount of pheromone which is proportional to the fitness of its solution. This process is iterated until the stopping criterion is satisfied.

## 4. Parametric Model Identification

### 4.1. Excitation signal

This work aims to obtain data with as much information as possible about the process under study and in a wide range of frequencies. According to Ljung [9], the type of input signal to be used should be able to excite all the dynamic modes of interest where the spectral content of the input signal should be rich in frequency corresponding to system bandwidth. It should also be rich in amplitude level whereby it should have different levels of input amplitudes over the whole range of operation. This goal can be achieved by exciting the process with a pseudo-random binary signal (PRBS). This signal will provide not only a persistent excitation to the process and rich in amplitude level, since input changes are applied to both up and down directions to evaluate possible nonlinearities and different gains. Experimental work is carried out using a sampling time of  $T = 0.1s$  and duration of 100 seconds. Input–output data necessary for parametric identification are collected, where the excitation signal input PRBS indicates the voltage of main rotor,  $u(t)$  is used to excite the TRMS system. The output data collected is the pitch angle of the beam,  $y(t)$ . The input PRBS and its power spectral densities are shown in Figure 3.

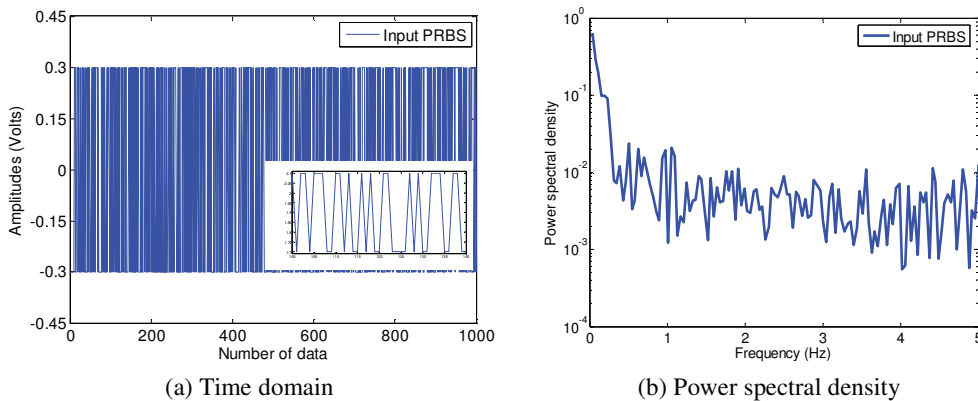


Figure 3: Pseudo random binary signal

### 4.2. Model structure

It has been observed from the power spectral density of the system that the significant mode lies in the 0-1Hz bandwidth, with a main resonance mode at 0.34Hz which can be attributed to the main body dynamics. A model order of 2, 4, and 6 corresponding to prominent normal modes at 0.25Hz, 0.34Hz, and 0.46Hz were anticipated. However, a fourth order model was employed which gave better representation of the system dynamics than a second or sixth order [10]. The parametric modeling technique employed in this paper is shown in Figure 4.

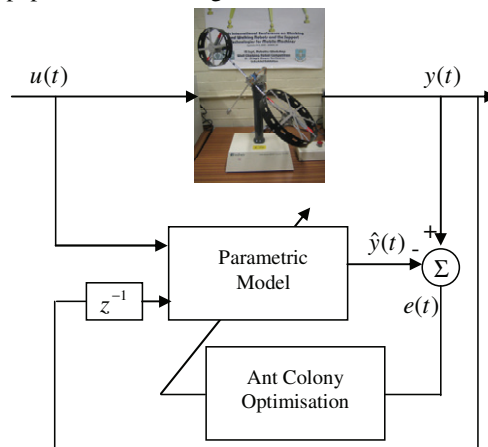


Figure 4: Parametric modeling of a TRMS

Auto-regressive with exogenous input (ARX) model structure is chosen, as depicted in Figure 3 for the parametric model and expressed as [9]

$$\hat{y}(t) = -\sum_{i=1}^N a_i \times y(t-i) + \sum_{j=0}^M b_j \times u(t-j) \quad (5)$$

where  $a_i, b_j$  are denominator and numerator polynomial coefficients,  $N$  and  $M$  are the number of coefficients in the denominator and numerator polynomials,  $y$ ,  $u$  and  $\hat{y}$  are measured output, input and predicted output respectively. The order of the transfer function depends on  $N$ . Taking the values of  $N$  and  $M$  as 4 and 3, equation (2.24) can be simplified as:

$$\hat{y}(t) = -a_1 y(t-1) - \dots - a_4 y(t-4) + b_0 u(t) + \dots + b_3 u(t-3) \quad (6)$$

A useful way to visualise equation (2.25) is to view it using a backshift operator  $z^{-1}$  as defined by

$$\hat{y}(t) = \left( \frac{b_0 z^{-1} + b_1 z^{-2} + b_2 z^{-3} + b_3 z^{-4}}{1 + a_1 z^{-1} + a_2 z^{-2} + a_3 z^{-3} + a_4 z^{-4}} \right) \quad (7)$$

The difference between the predicted and actual output is recorded as error,  $e(t)$ :

$$e(t) = y(t) - \hat{y}(t) \quad (8)$$

## 5. Model validation

It is crucial to test that the identified model can adequately describe the data set in any model formulation or algorithm identification [11]. In practise, the model of the system will be unknown and the detection of an inadequate fit is more challenging.

### 5.1. One step ahead prediction

The one-step-ahead (OSA) prediction of the system output is a common measure of predictive accuracy used in control and system identification [12]. This approach is adopted in this work and expressed as:

$$\hat{y}(t) = f[u(t), u(t-1), u(t-2), \dots, u(t-n_u), y(t-1), y(t-2), \dots, y(t-n_y)] \quad (9)$$

where  $f(\bullet)$  is a nonlinear function,  $u$  and  $y$  are the input and output respectively. The residual or prediction is the difference between the measured output and the predicted output, given by:

$$e(t) = y(t) - \hat{y}(t) \quad (10)$$

Often  $\hat{y}(t)$  will be a relatively good prediction of  $y(t)$  over the estimation set even if the model is biased because the model was estimated by minimizing the prediction errors.

### 5.2. Correlation tests

Apart from OSA prediction, correlation tests are convincing methods in model validation. These tests not only give information on the quality of the model structure being investigated, but also indicate bias to noise. If a model is adequate, then the residuals or prediction errors  $e(t)$  should be unpredictable from all linear and nonlinear combinations of past inputs and outputs. The derivation of simple tests that can detect these conditions is complex, but it can be shown that the following conditions should hold [11].

$$\phi_{ee}(\tau) = E[\varepsilon(t-\tau)e(t)] = \delta(\tau) \quad (11)$$

$$\phi_{ue}(\tau) = E[u(t-\tau)e(t)] = 0 \quad \forall \tau \quad (12)$$

$$\phi_{u^2e}(\tau) = E[(u^2(t-\tau) - \bar{u}^2(t))e(t)] = 0 \quad \forall \tau \quad (13)$$

$$\phi_{u^2e^2}(\tau) = E[(u^2(t-\tau) - \bar{u}^2(t))e^2(t)] = 0 \quad \forall \tau \quad (14)$$

$$\phi_{e(eu)}(\tau) = E[e(t)e(t-1-\tau)u(t-1-\tau)] = 0 \quad \tau \geq 0 \quad (15)$$

where,  $\phi_{ee}(\tau)$ , the auto-correlation of the residuals in equation (11) should be an impulse, and  $\phi_{ue}(\tau)$ , the cross-correlation functions in equations (12) – (15) should ideally be zero. Ideally, the model validity tests should detect all the deficiencies in the algorithm performance including bias due to internal noise. The cause of the bias will however be different for different assignments of input set. Correlation function between two sequences  $\psi_1(t)$  and  $\psi_2(t)$  is given by:

$$\hat{\phi}_{\psi_1\psi_2}(\tau) = \frac{\sum_{t=1}^{N-\tau} \psi_1(t)\psi_2(t+\tau)}{\sqrt{\sum_{t=1}^N \psi_1^2(t) \sum_{t=1}^N \psi_2^2(t)}} \quad (16)$$

In practise, normalised correlations are computed. Normalisation ensures that all the correlation functions lie in the range  $-1 \leq \hat{\phi}_{\psi_1\psi_2}(\tau) \leq 1$  irrespective of the signal strengths. The correlation will never be exactly zero for all lags and the 95%

confidence band defined as  $\frac{1.96}{\sqrt{N}}$  is used to indicate if the estimated correlation is significant or not, where  $N$  is the length

of data. Therefore, if the correlation function is within the confidence interval, the model is regarded as adequate. Among the five correlation tests, equations (11) and equations (12) are generally used to determine model validity in the case of linear modelling, whereas all the five equations (11) to (15) are used in the case of nonlinear modelling.

### 5.3. Percentage accuracy

Accuracy of a result or experimental procedure can refer to the percentage difference between the experimental result and the accepted value. In this work, the percentage of accuracy is calculated to measure the relationship between the actual output  $y(t)$  and predicted output  $\hat{y}(t)$  according to equation (10). Closer value of percentage accuracy to 100% replicates an accurate time domain output mapping of actual output and predicted model output of the system.

Percentage accuracy = 100% - Percentage error

$$= \left( 1 - \left( \frac{1}{N} \sum_{t=1}^N \frac{y(t) - \hat{y}(t)}{y(t)} \right) \right) \times 100 \quad (17)$$

## 6. Results and Discussions

All simulations were carried out on a PC (Intel Pentium @, 2.30 GHz, RAM 3.50 GB). The predicted output for time-domain tracking using ACO algorithm for vertical motion is presented against the actual measured output in Figure 5(a). This result is shown as function of data points, where the spacing between successive data points is 0.1sec. It is clearly evident that the algorithm predicted the pitch movement very well. The accuracy between the actual and predicted output is 99.33%. For frequency-domain response, the result is presented in Figure 5(b). It is apparent that the derived model could follow the actual system dynamics in the low frequency region, whereas some differences were observed at higher frequency region which were not significant as far as the twin rotor system operation is concerned. The pole-zero diagram of the system model using the proposed method is presented in Figure 5(c). It is noted that the poles and zeros were inside the unit circle using ACO technique. Figure 5(d) shows the convergence towards the smallest error value for modeling optimisation using ACO algorithm. It is clearly evident that the convergence curves remain static with small improvements

after 230 iterations for the ACO algorithm. It is noted that ACO algorithm has achieved good MSE value at 757 iterations. The maximum number of iterations was set to 1000 for each algorithm.

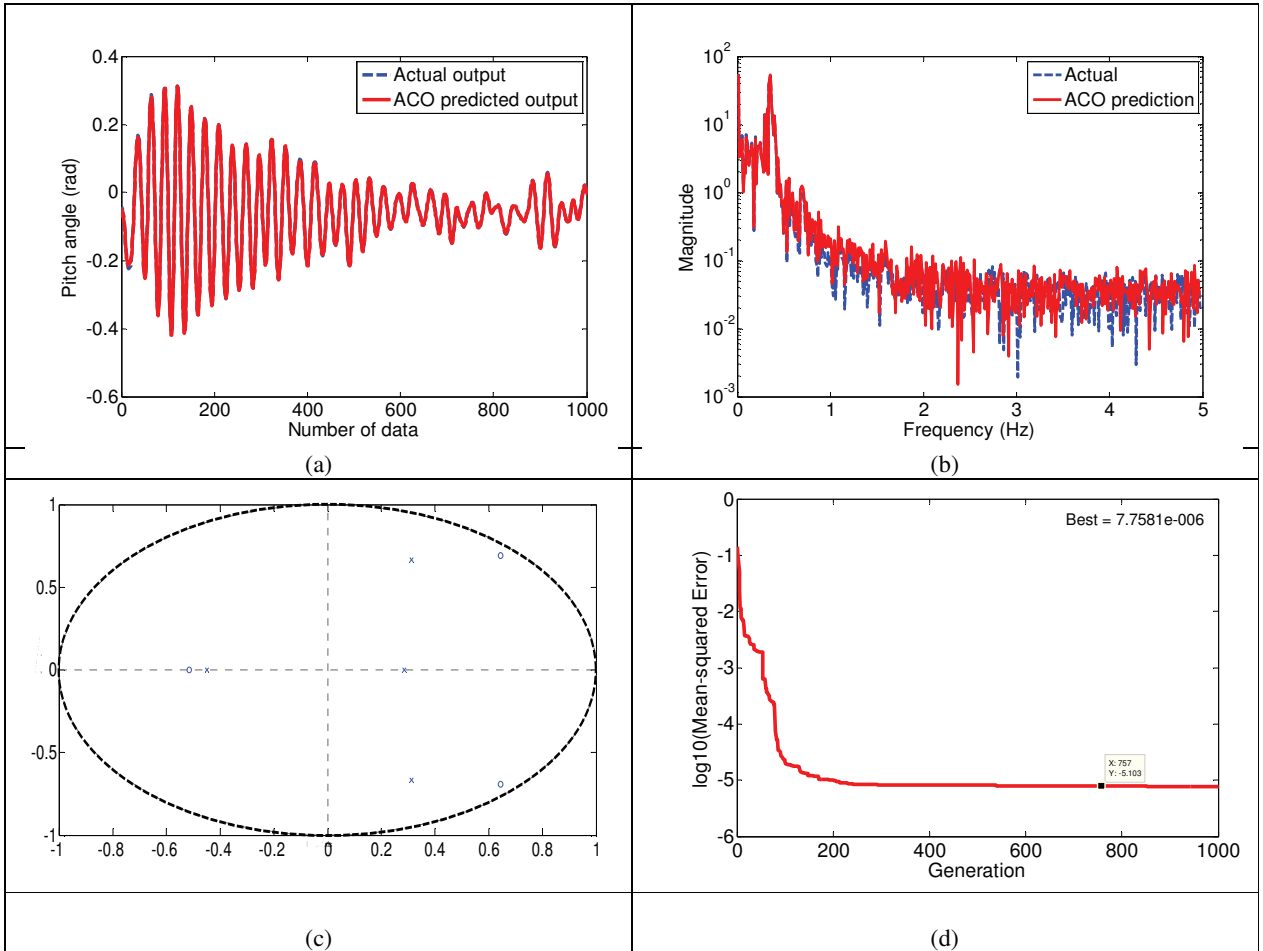


**Figure 5:** a) Actual and ACO predicted output of the system, b) Power spectral density of actual and ACO predicted output, c) Pole zero diagram of the system, d) Convergence diagram for 1000 iterations using ACO

Using the steps in ACO algorithm, the combination of  $a_i$  and  $b_i$  that give the smallest mean-squared error (MSE) of  $e(t)$  were optimized using the following parameter setting as depicted in Table 2.

**Table 2:** Parameters setting

Archive size, $k$	40
Number of ants used in an iteration, $m$	20
Locality of serach process, $q$	1e-1
Simulation time, $t$	100s
Speed of convergence, $\xi$	0.9
Number of parameters (based on eqn. (7))	8



Correlation validations of vertical plane motion model are shown in Figure 6. It is noted that all the five correlation functions were within the 95% confidence bands interval with 1000 data pairs. This indicates that the model behavior was unbiased and close to that of the real system.

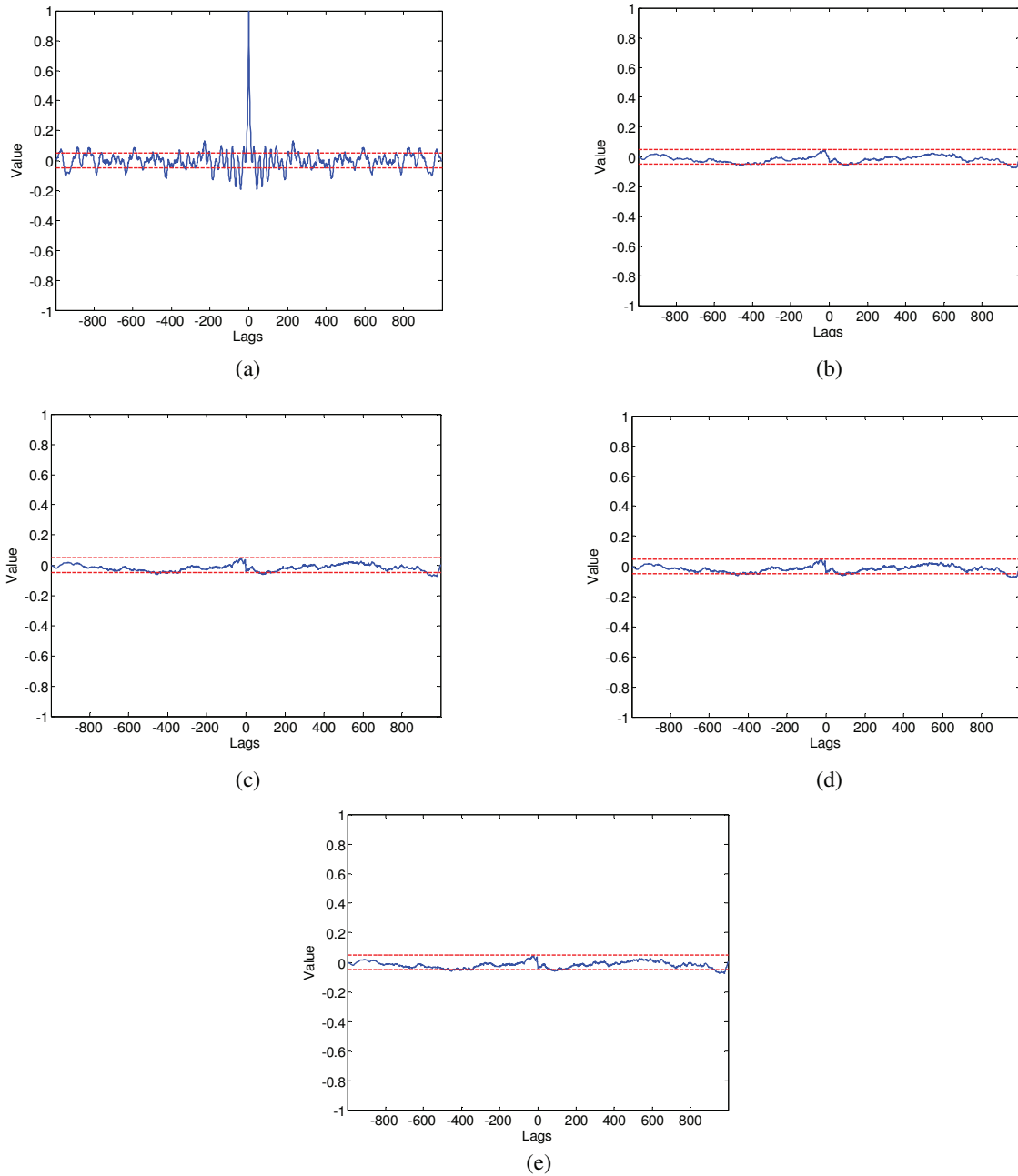


**Figure 6:** Correlation test of RLS estimation: a) Auto-correlation of residuals, b) Cross-correlation of input and residuals, c) Cross-correlation of input square and residuals, d) Cross-correlation of input square and residual square, e) Cross-correlation of residual and (input\*residuals)

## 7. Conclusion

The system identification problem has been formulated as an optimization task in which ant colony optimization has been used to estimate parameters of the TRMS so as to minimize the prediction error between actual and predicted outputs at each time step. It is also evident that the algorithm can extract a stable and satisfactory model for the system. This indicates in-built robustness of the algorithm which can be equally useful and applicable to other systems. The potential of the ACO modeling can be further explored for control strategy optimization based on twin rotor application.

## References

- [1] Dorigo, M., Caro, G. D. and Gambardella, L. M. (1999). Ant algorithms for discrete optimization. *Artificial Life*, 5, (2), 137-172.
- [2] Bennett, P. J., Pearson, J. I., Martin, A., Dixon, R., Walsh, M. C., Khella, M., (2006), Application of diagnostic techniques to an experimental aircraft fuel rig, Sixth IFAC Symposium on Fault Detection, Supervision and Safety of Technical Processes, Tsinghua University, P.R. China, Aug 29 - Sept 1<sup>st</sup>.
- [3] Werner H., (1996), "Robust control of a laboratory flight simulator by non-dynamic multirate output feedback", IEEE Conference on Decision and Control, Kobe, Japan, 1575-1580.
- [4] Oberoi, S. (2004), Robust control of a laboratory scale launch vehicle model using fast output sampling technique, 5<sup>th</sup> Asian Control Conference, 20-23 July, Melbourne, Australia, 383-391.
- [5] Chen L., Shen J., Qin L., and Chen H. J. (2003) An improved ant colony algorithm in continuous optimization, *Journal of Systems Science and Systems Engineering*, 12 (2), 224-235.
- [6] Socha K. and Dorigo M. (2008), Ant colony optimization for continuous domain, *European Journals of Operational Research*, **185** (3), 1155-1173.
- [7] Wang L. and Wu Q. (2001) Ant system algorithm for optimization in continuous space, *Proceedings of the IEEE International Conference on Control Applications*, 395-400.
- [8] Quan H. and Chao H. (2007) Satellite Constellation Design with Adaptively Continuous Ant System Algorithm, *Chinese Journal of Aeronautics*, 20 (4), 297-303.
- [9] Ljung, L. (1999). *System identification: theory for the user*, Englewood Cliffs, New Jersey, Prentice-Hall.
- [10] Ahmad, S., Chipperfield, A. and Tokhi, M. (2001). Parametric modelling and dynamic characterization of a two-degree-of-freedom twin-rotor multi-input multi-output system. *Proceedings of the Institution of Mechanical Engineers, Part G: Journal of Aerospace Engineering*, 215, (2), 63-78.
- [11] Billings, S. A. and Zhu, Q. M. (1994). Nonlinear model validation using correlation tests. *International Journal of Control*, 60, (6), 1107 - 1120.
- [12] Shaheed, M. H. (2005). Feedforward neural network based non-linear dynamic modelling of a TRMS using RPROP algorithm. *International Journal on Aircraft Engineering and Aerospace Technology*, 77, (1), 13-22.